BEAM INDUCED FLUORESCENCE - PROFILE MONITORING FOR TARGETS AND TRANSPORT

F. Becker*, C. Andre, C. Dorn, P. Forck, R. Haseitl, B. Walasek-Hoehne, GSI, D-64291 Darmstadt
T. Dandl, T. Heindl, A. Ulrich, Physik Department E12 TU-München, D-85748 Garching
J. Egberts, J. Marroncle, T. Papaevangelou, Centre CEA de Saclay, F- 91191, France

Abstract

Online profile diagnostic is preferred to monitor intense hadron beams at the Facility of Antiproton and Ion Research (FAIR). One instrument for beam profile measurement is the gas based Beam Induced Fluorescence (BIF)-monitor. It relies on the optical fluorescence of residual gas, excited by beam particles. In front of production targets for radioactive ion beams or in plasma physics applications, vacuum constraints are less restrictive and allow a sufficient number of fluorescence photons, even at minimum ionizing energies. Unwanted effects like radiation damage and radiation induced background need to be addressed as well. A profile comparison of BIF and Ionization Profile Monitor (IPM) in nitrogen and rare gases is presented. We studied the BIF method from 10^{-3} to 30 mbar with an imaging spectrograph. Preferable fluorescence transitions and fundamental limitations are discussed.

MOTIVATION

Compared to synchrotrons with typical vacuum pressures p_{SYN} of $1{\cdot}10^{-12}$ to $1{\cdot}10^{-9}$ mbar, beam transport sections are usually operated in the range p_{TS} of $1{\cdot}10^{-9}$ to $1{\cdot}10^{-6}$ mbar. This fact increases the set of possible instrumentation in the FAIR HEBT sections, since the expected signal strength for gas based profile monitors scales $\propto p$, see [1, 2]. Beside Ionization Profile Monitors (IPMs) with MCP amplification for high sensitivity or applications with high read out rates [3], compact BIF installations or strip line IPMs are foreseen. Within a collaboration between CEA-Saclay and GSI-BD an IPM prototype, designed for the IFMIF/EVEDA facility [4] was characterized at the GSI LINAC experimental branch for various beam and gas conditions [5]. Together with the IPM a BIF monitor was installed in the same plane and profiles of a 1.1 mA Xe^{21+} beam with 250 μs pulse length @ 4.8 MeV/u were recorded in nitrogen and rare gases.

At low duty cycles, temporarily triggered gas puffs beyond $1{\cdot}10^{-4}$ mbar could be provided with pulsed gas valves. In front of production targets for radioactive ion beams or in plasma physics applications, vacuum requirements are less restrictive or even protective gases are used with typical pressures p_{TAR} from $1{\cdot}10^{-4}$ mbar to atmospheric pressure. In order to characterize the BIF monitor at gas pressures $\geq 1{\cdot}10^{-4}$ mbar, imaging spectroscopy was performed in a separated gas cell at the Munich Tandem van de Graaff accelerator. With a DC 200 nA S^{8+} beam at 3.75 MeV/u former results [6] for gas pressures $\leq 1{\cdot}10^{-3}$ mbar could be confirmed. This data-basis was now extended to gas pressures up to 30 mbar.

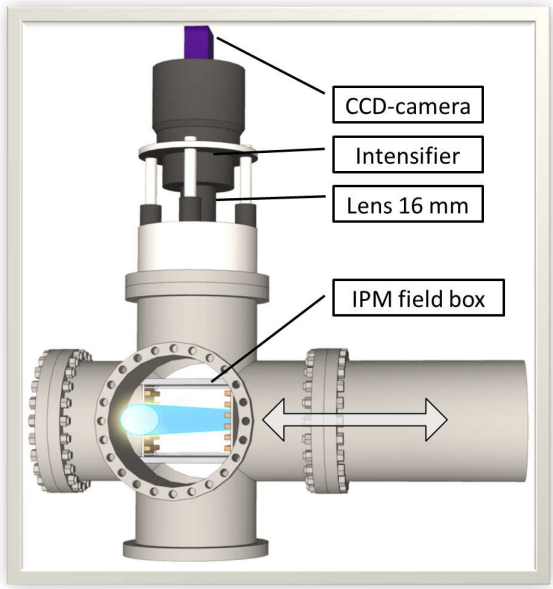

Figure 1: Schematic drawing of the experimental setup with the IPM and BIF monitor mounted in the same plane on a blackened vacuum chamber (DN100CF). The IPM field box could be moved out the chamber with a stepper motor controlled linear drive (to the left).

BIF IPM - EXPERIMENTAL SETUP

In order to compare horizontal profiles of the different monitors, we decided to place both systems in the same transversal plane, see Fig. 1. During IPM operation the electric field box was centered in the chamber and moved out of the optical path for BIF operation. The vacuum chamber was sandblasted and blackened by electrochemical surface treatment to suppress stray-light from the chamber walls during BIF operation. The experimental branch is equipped with a 700 l/s turbomolecular pump and reaches a typical base pressure of $2{\cdot}10^{-7}$ mbar. Furthermore, it is equipped with a remote controlled gas dosing system. This way, purified gases (e.g. nitrogen and rare gases) could be applied in a dynamic equilibrium within an accessible pressure range from 10^{-6} to 10^{-3} mbar. For cleaning purpose during gas exchange, the vacuum system was evacuated to base pressure.

The IPM illustrated in Fig. 1, consists of a 55x61 mm^2 field box with 833 V/cm electric field for ion detection and

* Frank.Becker@gsi.de

ISBN 978-3-95450-118-2

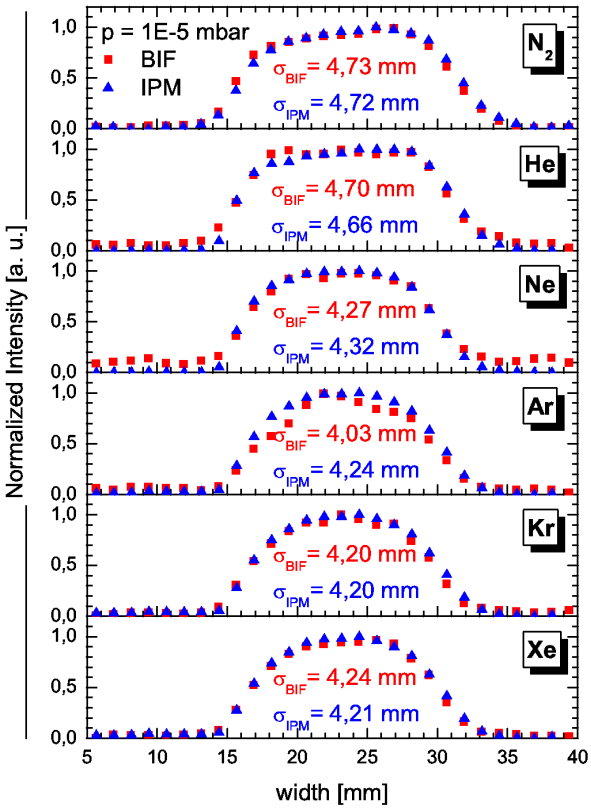

Figure 2: Normalized beam profiles (BIF and IPM) in different gases at $\geq 10^{-5}$ mbar (averaged over 300 Xe21+-pulses of 1.1 mA and 250 μs pulse length). 172 BIF pixels were smoothed with a 20 points 3^{rd}-order Savitzky-Golay filter and interpolated to the 32 IPM-channels (28 displayed here). σ was calculated within 15-35 mm ROI.

simulated field inhomogeneities below 4 %. It is a non-intensified system with electrical read out: 32 metalized stripes with 1.25 mm interspacing cover an active area of 10x40 mm. They are connected to trans-impedance, integrating or logarithmic amplifiers and the amplified signal is then multiplexed to an 8-bit 1 GHz ADC. All mechanical parts, HV settings and DAQ were remote controlled.

The BIF monitor installed in the setup was realized as MCP-based image intensifier in V-stack configuration, coupled to a CCD camera. The image intensifier provides 33 lp/mm spatial resolution and is equipped with a bi-alkali photo cathode. A remote controlled reverse voltage in the intensifier unit allowed a precise setting of the integration time (down to 100 ns with $\leq$ 1 ns time base jitter). Data acquisition was carried out with a digital half inch, CCD camera in 8-bit gray scale VGA resolution. The camera control and read-out were realized via FireWire interface and the highly flexible BeamView user interface [7]. The used lens system has 16 mm focal length and a maximum aperture of κ = 1.4. It is equipped with a remote controlled iris with κ 1.4-22 in order to cover the dynamic range of the experiment. The optical assembly has a spectral sensitivity of 390 to 550 nm and was installed 20 cm to the center of the chamber (object distance). In this configuration a spatial resolution of 230 μm/pixel was realized.

PROFILE ANALYSIS - RESULTS

Profile data of both systems were analyzed for identical spatial regions and matching statistical increments. This is achieved by an experimental setup allowing both monitors to observe the beam at the same time for calibration purpose. During that procedure, the IPM field box is placed beneath the intensified imaging system (BIF). The shadings of the IPM field box, namely 31 cut out interspaces between the read out strips, allow precise calibration of the BIF (active area: 43x153 pixels comply with 10x36 mm). Statistical increments are matched by resizing the CCD projection vectors to 32 bins, in order to match the 32 IPM read-out strips.

Both monitors worked reliably for 1.7 mA U^{28+} and 1.1 mA Xe^{21+}-beams @ 4.8 MeV/u from 10^{-6} to 10^{-3} mbar. As compared to the BIF monitor, the IPM is about one order of magnitude more sensitive. However the intensified CCD with bi-alkali photocathode showed a negligible number of dark counts and therefore a superior SNR. For 10^{-5} mbar, beam profiles recorded with the different detectors agree very well for the investigated gases, see Figure 2. Relative differences in the recorded beam width σ are below 5 %. A slight energy drift during the six hours machine run might be the reason for decreasing beam width from N_2 to Xe. More details about this experiment can be found in [5]. For increasing gas pressures, recorded beam profiles were broadened and BIF profiles deviate from the IPM data. Especially BIF profiles in He were significantly broadened, see also [6]. This stresses the necessity for further spectroscopic research for p $\geq 10^{-3}$ mbar.

SPECTROSCOPIC SETUP

The desired pressure range from 10^{-3} mbar to atmospheric pressure requires a customized vacuum system with high flexibility. We decided for a gas cell, separated by a vacuum window and turbomolecular pump that could be bypassed during p $\geq 5{\cdot}10^{-3}$ mbar applications. Figure 3 illustrates the gas cell with a 1.1 mg/cm^2 and ø 5 mm Ti-window (A) to separate the vacuum system of the transport section. Two equally spaced (20 mm) steel plates (B) and (C) with ø 10 mm core holes, have been isolated from the chamber grounding. For the right potential, the plates worked as repeller anode for secondary electrons from (U_A= -1000V, U_B= 0V). However, no significant influence on the actual imaging spectroscopy data was observed. Presented spectroscopic results in this contribution were recorded with potential plates grounded.

Investigated gases (N_2, Xe, Ar, Ne, He) with a purity better than 99.998 % have been applied in a dynamic equilibrium at permanent flow against a 700 l/s turbomolecular pump for p $\leq 5{\cdot}10^{-3}$ mbar and against a 12 m^3/h scroll compressor in a bypass mode for higher pressures. Between two different gas species, the chamber was evacuated to $2{\cdot}10^{-7}$ mbar base pressure for cleaning purpose. Measurements with a residual gas analyzer confirm impurities $\leq$ 1 ‰.

ISBN 978-3-95450-118-2

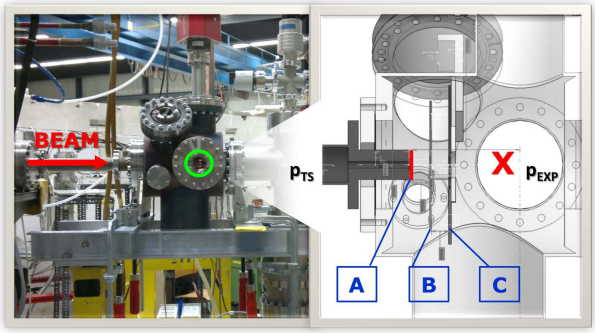

Figure 3: Photograph of the installations (left) and zoomed technical drawing of the chamber setup (right). The red cross indicates the optical sweet spot of the imaging spectrograph. The experimental cell with a gas pressure of p_{EXP} is separated by a Ti-window (A) from the vacuum system of the transport section at p_{TS}. The HV-plates (B) and (C) could be set to dedicated potentials.

The imaging spectrograph with ∼1.5 nm spectral resolution, described in [6] was mounted in front of the CF-40 view port (optical grade, fused silica), see Fig. 3 (green). According to the calibration, the reproduction scale was measured to be 492 pixel per 15 mm (≙ 30 μm/pixel) in the spatial dimension and 656 pixel per 533 nm (within 260 and 793 nm) in the spectral dimension. Spatial calibration and focusing was realized with a row of four LEDs with 0.2 mm diameter and 5 mm interspacing, that were pneumatically moved to the beam axis. For spectral calibration, a Hg-Ar lamp, coupled to a UV-grade fiber was fed into the vacuum chamber and mounted on the movable calibration holder. Measurements in this publication were recorded with 5 μm entrance slit opening. The spectral efficiency of the optical system is shown in Fig. 4. Depth of field was calculated to be 2, 4 and 16 mm for f-stop 2.8, 5.6 and 22, focal distance f=50 mm, blurring diameter z=30 μm and g=200 mm object distance [2].

For data acquisition, an image intensified digital camera (ICCD), equipped with a bialkali photocathode and a two stage MCP configuration was used [6] - the same system used for the profile comparison.

SPECTROSCOPIC ANALYSIS - RESULTS

In order to cover the full dynamic range of 5.3 orders of magnitude (∼55 dB) for increased gas pressure from $1{\cdot}10^{-4}$ to 30 mbar, the ICCD camera was operated in a photon counting mode. Assuming 2 % of the 322 kpixel are counted during a full scale integration, a dynamic range of 38 dB is available. Another 18 dB were obtained by fading down the iris from f-stop 2.8 to 22. Each set of parameters was recorded as sequence of 1000 images with 170 ms integration time and 5 Hz rep rate, for constant accelerator settings (DC 200 nA S^{8+} @ 3.75 MeV/u). The images were analyzed with an ImageJ algorithm, assigning local grayscale maxima to corresponding pixels [2]. Typical image blurring due to intensifier blobs could be avoided this way. Electronic noise from the CCD was suppressed by a 3 bit threshold. Furthermore, hot pixel were identified and excluded. Processed image data is nearly noiseless and contains a negligible number of dark counts.

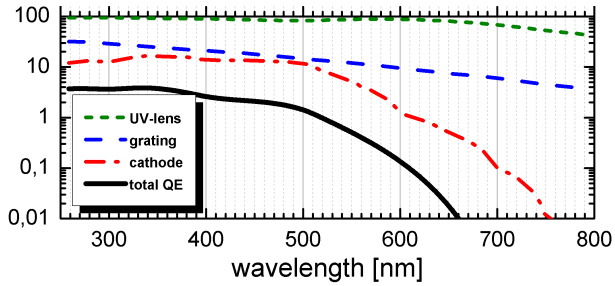

Figure 4: Spectral efficiencies of the relevant optical components and their product (black). Viewport and photocathode substrate show flat response within 250 - 800 nm.

Depending on the experimental purpose, either spectral (Fig. 5) or spatial (profile) information (Fig. 6) was obtained from the fluorescence images. By choosing confined Regions Of Interest (ROI), even profiles of single atomic transitions (Fig. 8), or spectra of a certain beam region can be displayed. A more detailed description of imaging spectroscopy in different workin gases can be found in [2].

Spectral Study

Fluorescence spectra were obtained from a 30 by 656 pixel core-ROI of the excited gas volume, which corresponds to 0.9 mm in the spatial dimension and 533 nm in the spectral dimension. In Fig. 5, fluorescence spectra of different working gases are plotted for three different pressures of the respective gas species.

Spectra of the particularly lowest gas pressure at $1{\cdot}10^{-3}$ mbar (solid lines) confirm former experimental data [6]. For intermediate pressures (dashed lines) a spectral conversion was observed, with different transitions appearing. For the particularly highest gas pressure (dotted lines) the spectral intensity of Xe, Ar and Ne is concentrated in a few or even a single transition. In He and N_2 there is no concentration, but totally different transitions were observed, compared to the low pressure case.

For low N_2 pressures, only transitions of the ionized molecule N_2^+ (B→X) were observed. In 30 mbar, transitions of the neutral N_2 (C→B) appeared exclusively. This strongly affects the profile reading, as transitions of the neutral molecule are now more likely excited by secondary electrons [8]. They tend to generate profile halos according to the additional mean free path of the electrons. In high He pressures beside two neutral transitions at 330 and 355 nm, a pronounced line appears exactly at at 391 nm, the N_2^+ (B→X) (0-0). The same line is observed for intermediate pressures in Ne and Xe and might be due to traces of nitrogen. Different transfer processes due to N_2 impurities can be observed in all rare gas species. In Ar a hydroxide transition (OH^*) at 310 nm was observed, which originates from dissociated water vapor in the unbaked system.

ISBN 978-3-95450-118-2

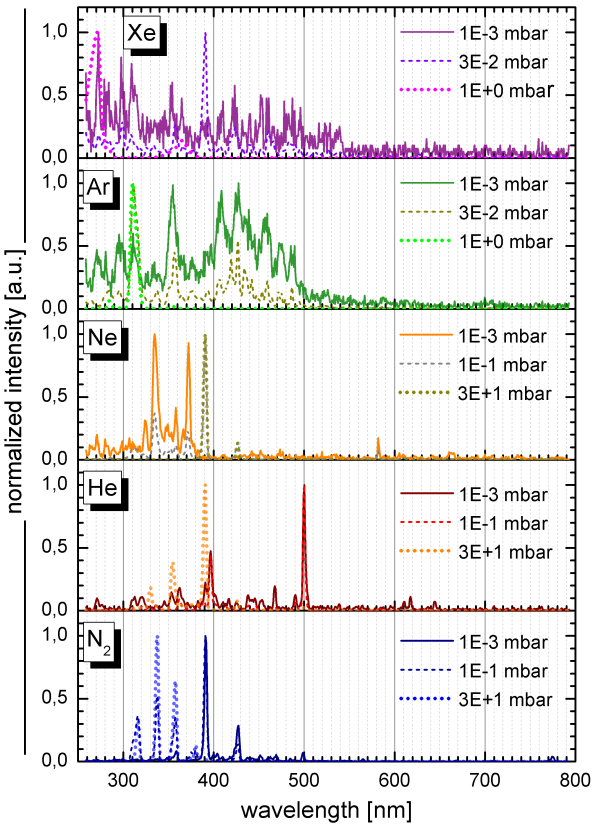

Figure 5: Normalized fluorescence spectra of a DC 200 nA S^{8+} beam @ 3.75 MeV/u in different working gases (Xe, Ar, Ne, He, N_2), measured at three different gas pressures each. Ar-spectra were recorded with 15 μm slit opening.

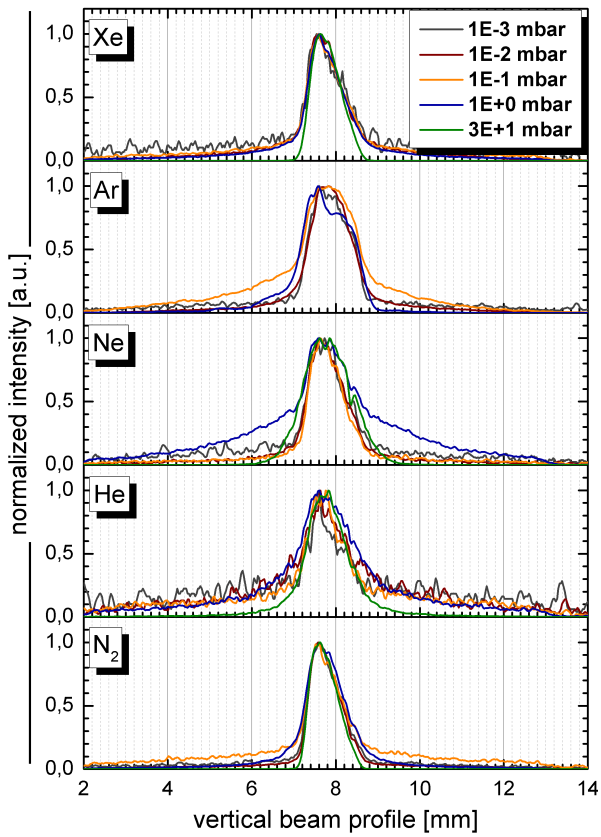

Figure 6: Normalized beam profiles in the working gases Xe, Ar, Ne, He and N_2, recorded at a set of different gas pressures each. Ar-profiles have been recorded with a different beam focusing.

Beam Profile Comparison

Beam profiles were obtained from full images in Fig.6 or from 492 by 10 pixel spectral region of interest, that corresponds to 15 mm in the spatial dimension and ~8 nm in the spectral dimension, in order to select profiles of specific transitions, see Fig. 8. The reader should be aware of possible drifts during 72 hours of operation. So, beam profiles of a respective gas species should only be compared among each others.

The profile data in Fig. 6 was recorded for constant accelerator settings but it should only be compared among a pressure series of the respective gas species, since drifts during 72 hours of operation cannot be ruled out.

Profile evaluation in Fig. 6 was done without spectral separation, taking into account all optical transitions within the spectral response, see Fig. 4. When gas pressure is increased, the observed beam profile width grows in all gas species. Beyond about $1{\cdot}10^{-1}$ mbar, beam profile width starts decreasing again. In N_2, He, and Xe, the narrowest beam profiles were observed for the highest gas pressure. However, the smallest relative change in profile width is clearly observed for nitrogen.

Figure 7 shows weighted standard deviations σ_w versus pressure for the beam profiles and gases of Fig. 6. All curves show decreasing σ_w for increasing pressure, with the smallest size for the highest pressure in each series. They also show a bump in the range of 10^{-2} to 10 mbar, which is visible in Fig 6 as well. One should be aware that no region of interest, smoothing or individual noise subtraction was applied and therefore beam sizes σ_w are convoluted with noise contributions from the profile edges for low pressures and inferior signal to noise ratio.

Transition selective beam profiles provide a deeper insight in the relevant processes. Figure 8 shows profiles of the most prominent transitions at 337 and 391 nm for increasing gas pressure. While profiles of the N_2 (C→B) (0-0) appear with the unwanted profile growth and decrease, the N_2^+ (B→X) (0-0) transition remains almost constant. In the other investigated gas species, this beneficial effect was observed for different optical transitions as well.

CONCLUSION

Beam profiles recorded with BIF monitors and IPMs agree very well for gas pressures below 10^{-4} mbar, see Fig. 2. Non intensified IPMs might be used whenever high sensitivity and robustness is required. BIF monitors will be selected, if compact dimensions are required, or space charge effects just would allow for IPMs with magnetic field guidance, see [3, 5]. However, for pressures above 10^{-4} mbar BIF profiles are broadened by secondary electrons. Just profiles of some ionic transitions are preserved.

ISBN 978-3-95450-118-2

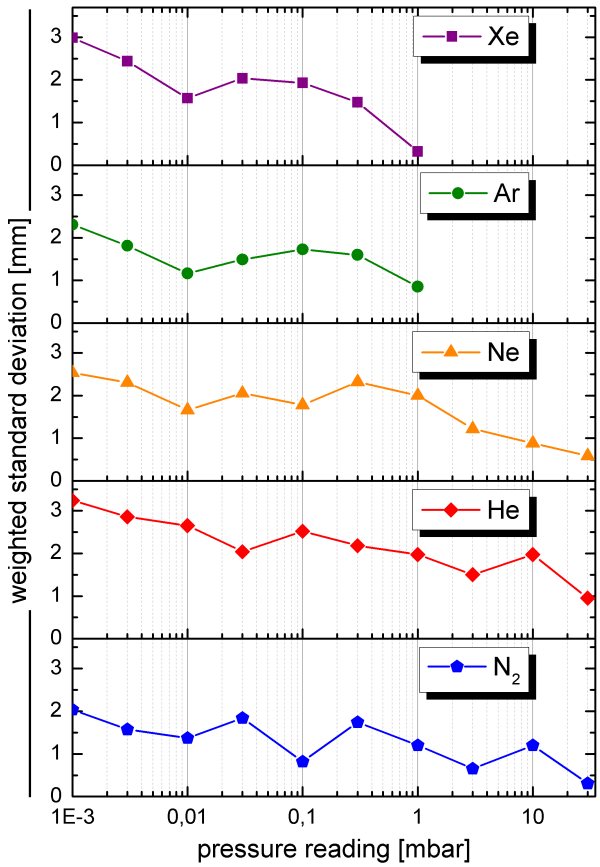

Figure 7: Weighted standard deviation σ_w of the beam profiles from Fig. 6. The complete profile from 2 to 14 mm was used for statistical calculation. Therefore the result is sensitive to noise contribution from the profile edges.

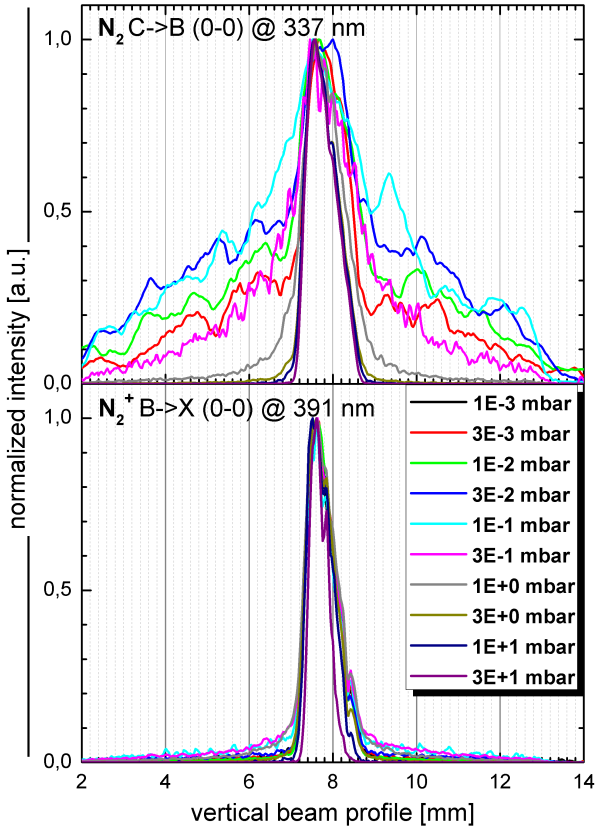

Figure 8: Normalized beam profiles of two selected nitrogen transitions for a set of increasing gas pressures each. The applied ROI selects one neutral and one ionic transition.

The observed bump in σ_w for increasing pressure in Fig. 6 and Fig. 7, is caused by a secondary electron fluorescence halo. Nevertheless, the exploitable dynamic range of BIF monitors can easily be extended to tens of millibars or even atmospheric pressure, as long as suitable transitions are selected with an optical filter. In the case of nitrogen, the N_2^+ B→X (0-0) at 391 nm should be selected, see Fig. 8 Usually ionic transitions seem to be profile preserving, in contrast to neutral transitions. In He no prominent ionic transition was observed. In Ne, Ar and Xe, fluorescence light of ionic transitions was divided among several lines. Further investigation is planned to provide a guideline for rare gases as well. Moreover, the excellent correlation with competitive profile monitors [5] makes BIF monitors a versatile instrumentation for FAIR applications.

ACKNOWLEDGEMENTS

We would like to express our sincere thanks to the E12 staff at TUM and the operator shifts, who made successful installation and measurements possible. This work could not have been realized without the invaluable help of H. Graf, S. Güttler and the GSI BD technicians with their ideas and support.

References

[1] P. Forck et al., "Beam induced fluorescence profile monitor developments," in *HB2010, Morschach*, WEO1C03, pp. 497–501, JACOW, 2010.

[2] F. Becker et al., "Beam induced fluorescence monitors," in *DIPAC, Hamburg*, WEOD01, pp. 575–579, JACOW, 2011.

[3] T. Giacomini et al., "Improving the reliability of an IPM", DIPAC'05 (POT004), Lyon, 2005, p. 150-152.

[4] A. Mosnier et al., "Development of the IFMIF/EVEDA accelerator", PAC'09 (TU2RAI01), Vancouver, 2009, p. 663.

[5] J. Egberts et al., "Detailed experimental characterization of an ionization profile monitor," in *DIPAC, Hamburg*, WEOA03, JACOW, 2011.

[6] F. Becker et al., "BIF monitor & Imaging spectrography of different working gases," in *DIPAC, Basel*, TUPB02 in -, pp. 161–163, JACOW, 2009.

[7] R. Haseitl et al., "BeamView - A data acquisition system for optical beam instrumentation," in *PCaPAC08, Jubiliana*, WEP006 in -, pp. 180–182, JACOW, 2008.

[8] A. Ulrich, "Lichtemission und Lasereffekt bei Anregung mit ionisierender Strahlung," in *Habilitationsschrift, Physik Department TU-München*, 1998.

ISBN 978-3-95450-118-2